Statistical characteristics of the observed Ly-α forest and the shape of the initial power spectrum

M. Demiański[1,2], A.G. Doroshkevich[3]

1. Institute of Theoretical Physics, University of Warsaw, 00-681 Warsaw, Poland
2. Department of Astronomy, Williams College, Williamstown, MA 01267, USA
3. Astro Space Center of Lebedev Physical Institute of Russian Academy of Sciences, 125047 Moscow, Russia

Abstract

We analyze basic properties of about 6000 Ly-α absorbers observed in high resolution spectra of 19 QSOs. We compare the observed characteristics with those predicted by our model of formation and evolution of dark matter (DM) structure elements based on the Zel'dovich theory. This model asserts that absorbers are formed in the course of both linear and nonlinear adiabatic or shock compression of DM and gaseous matter. Using the probability distribution functions resulting from our model we link the observed separations and the DM column density of absorbers with the correlation function of the initial velocity field. Using our sample of absorbers we recover the CDM like power spectrum of initial density perturbations at scales $10h^{-1}$ Mpc $\geq D \geq 0.15h^{-1}$ Mpc with a precision of $\sim 15\%$. At scales $\sim 3 - 150h^{-1}$kpc the measured and CDM-like spectra are different. This result suggests a possible complex inflation with generation of excess power at small scales.

1 The database.

In our analysis we use 19 high resolution spectra which contain 7 770 absorbers. For detailed investigation we selected a more homogeneous sample of 6 270 absorbers with $b \geq 5$ km/s such that their measurement errors are restricted by $\Delta \log N_{HI} \leq 0.2$ and $\Delta b \leq 0.3b$.

2 Observed characteristics of absorbers

For the selected sample the redshift distribution of absorbers and redshift dependence of their basic observed mean characteristics, the Doppler parameter $< b >$, the hydrogen column density $< \log(N_H I/{z_4}^2) >$, and their mean separation $< d_{sep}{z_4}^2 >$, where $z_4 = (1+z)/4$ are shown in Fig. 1.

These variations are well fitted by

$$\langle\log(N_{HI}/z_4^2)\rangle = 13.3 \pm 0.08,$$
$$\langle b\rangle = (26 \pm 2.1)\text{km/s}, \quad z_4 = (1+z)/4\,, \tag{1}$$
$$\langle d_{sep}z_4^2\rangle = (1.3 \pm 0.15)h^{-1}\text{Mpc} = (4 \pm 0.3)\cdot 10^{-2} l_v\,,$$

where l_v is the coherence length of the velocity field.

The observed probability distribution functions, PDFs, for the Doppler parameter, $P(b)$, the hydrogen column density, $P(N_{HI}/z_4^2)$, and the absorbers separation, $P(d_{sep}z_4^2)$, are plotted in Fig. 2. This choice of variables takes care of the redshift evolution of the considered here characteristics of absorbers.

These PDFs are well fitted by exponential functions

$$P(x_{HI}) \approx 0.4\exp(-0.8x_{HI}) + 2.9\exp(-5x_{HI})\,,$$
$$P(x_b) \approx \begin{cases} 0.15\exp(2.8x_b), & \text{b} \le b_{rap}, \\ 0.9\exp(-2.3x_b), & \text{b} \ge b_{rap}, \end{cases} \tag{2}$$
$$P(x_s) \approx 2.7\exp(-1.6x_s)[1 - 0.93\exp(-1.45x_s)]\,,$$
$$x_b = \frac{b}{\langle b\rangle}, \quad x_{HI} = \frac{N_{HI}/z_4^2}{\langle N_{HI}/z_4^2\rangle}, \quad x_s = \frac{d_{sep}z_4^2}{\langle d_{sep}z_4^2\rangle}\,,$$

where again $z_4 = (1+z)/4$ and $b_{rap} \approx 23.5 km/s$ discriminates between absorbers situated within rapidly and moderately expanded regions.

From these results it follows that:

1. Regular redshift variations of the mean observed characteristics of absorbers (see Fig. 1) and weak redshift dependence of PDFs (see Fig. 2) indicate the self similar character of absorbers' evolution over the whole range of redshifts under consideration. So, we can conclude, that at these redshifts the evolution is dominated by a balanced action of the same physical factors.

2. Both the mean absorbers separation $\langle d_{sep}z_4^2\rangle$ and its PDF, $P(x_s)$, coincide with the expected one derived for Gaussian initial perturbations with the amplitude $\sigma_8 \approx 0.9$.

3. The complex form of the PDF, $P(b)$, confirms that absorbers have been formed within both rapidly and moderately expanded regions. Analysis

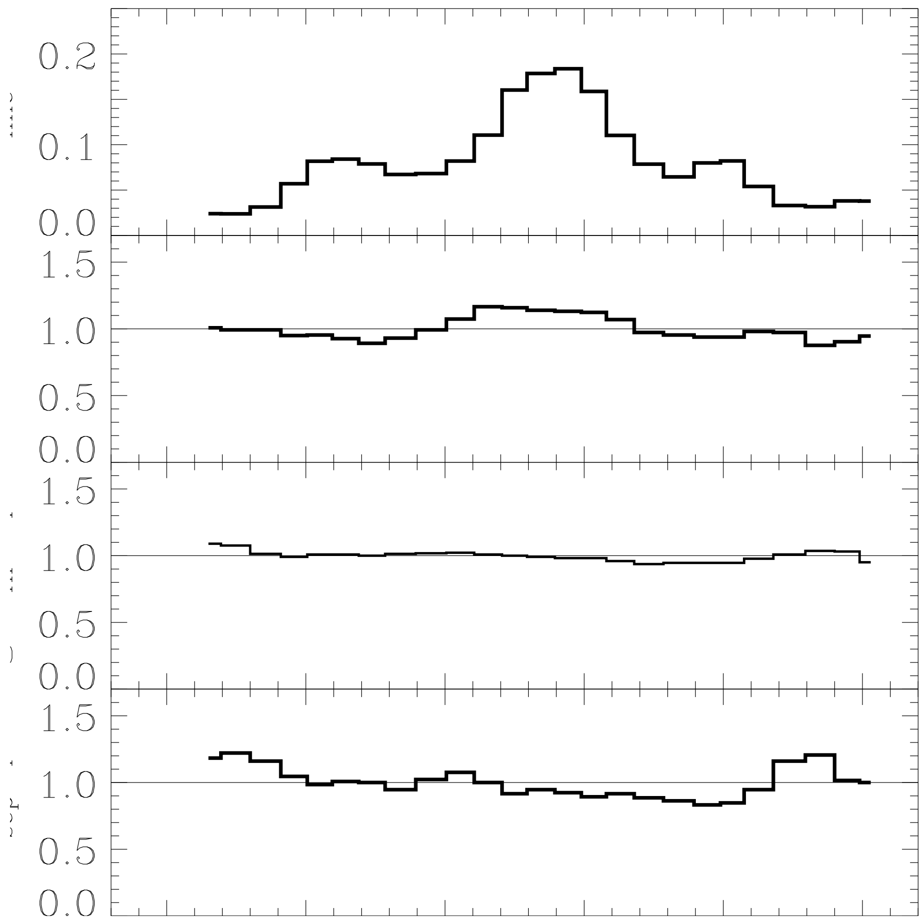

Figure 1: Redshift variations of fraction of measured absorbers, $f_{line} = \Delta N_{abs}(z)/N_{abs}$, (top panel), mean Doppler parameter, $\langle b(z)\rangle$ and HI column density, $\langle \lg(N_{HI} z_4^{-2})\rangle$ (two middle panels), and the mean absorber separation, $\langle d_{sep} z_4^2\rangle$ (bottom panel). All functions are normalized over their mean values.

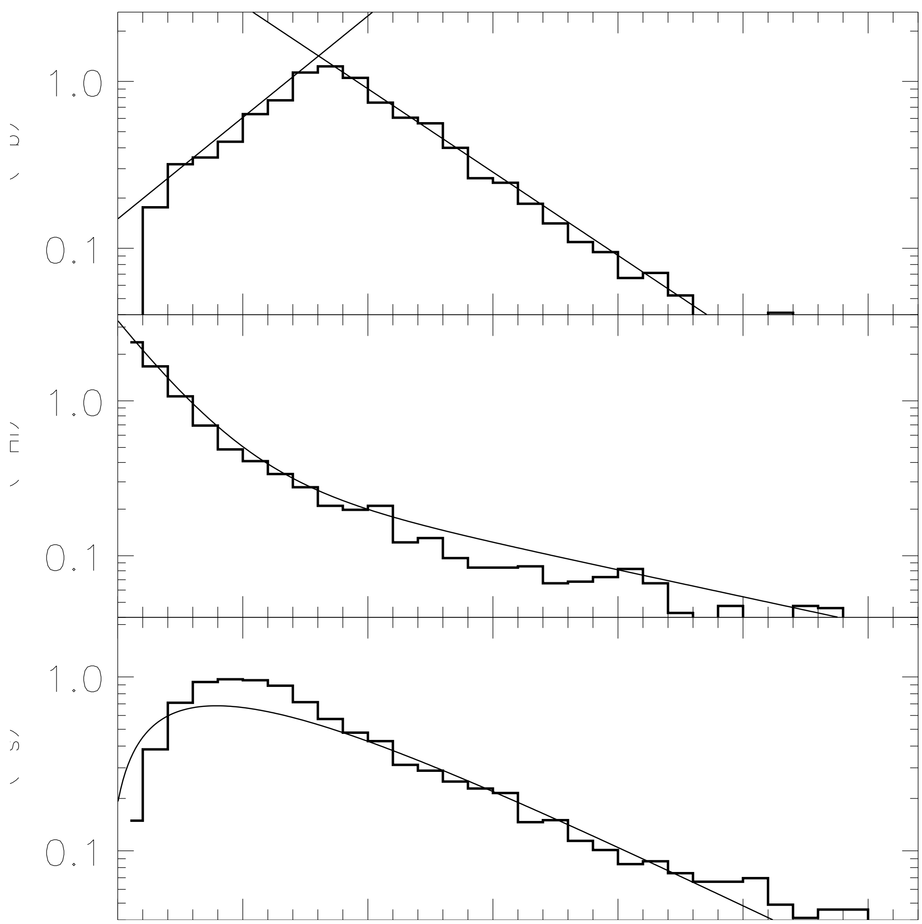

Figure 2: Observed PDFs for the Doppler parameter, $P_{obs}(x_b)$, the hydrogen column density, $P_{obs}(x_{HI})$, and absorbers separations, $P_{obs}(x_s)$, are plotted together with fits (2) (solid lines).

of these subpopulations of absorbers allows one to estimate some parameters of such regions.

4. The very wide range of measured Doppler parameters, $0.2 \leq b/b_{bg} \leq 5$, indicates a wide variety of initial perturbations. Formation of hotter and colder absorbers cannot be described in the framework of mildly nonlinear theory or by the model of "Fluctuating Gunn–Peterson Approximation" (discussed, e.g., in McDonald et al. 2004). Such a wide range of Doppler parameters is also not reproduced in simulations (Meiksin et al. 2001).

3 Correlation functions of the initial velocity field

3.1 The initial power spectrum and correlation functions of the initial velocity field

In our analysis we consider the spatially flat ΛCDM model of the Universe with the Hubble parameter and mean density given by:

$$H^2(z) = H_0^2\Omega_m(1+z)^3[1+\Omega_\Lambda/\Omega_m(1+z)^{-3}]\,,$$
$$\langle n_b(z)\rangle = 2.4\cdot 10^{-7}(1+z)^3(\Omega_b h^2/0.02)\mathrm{cm}^{-3}\,, \tag{3}$$
$$\langle\rho_m(z)\rangle = \frac{3H_0^2}{8\pi G}\Omega_m(1+z)^3, \quad H_0 = 100h\,\mathrm{km/s/Mpc}\,.$$

Here $\Omega_m = 0.3\,\&\,\Omega_\Lambda = 0.7$ are the dimensionless matter density and the cosmological constant (dark energy), Ω_b is the dimensionless mean density of baryons, and $h = 0.7$ is the dimensionless Hubble constant.

As a reference power spectrum of initial perturbations we take the standard CDM–like spectrum with the Harrison – Zel'dovich asymptotic,

$$P(k) = \frac{A^2 k}{k_0^4}T^2(\eta)D_W(\eta), \quad \eta = \frac{k}{k_0}, \quad k_0 = \frac{\Omega_m h^2}{\mathrm{Mpc}}\,, \tag{4}$$

where A is the dimensionless amplitude of perturbations, k is the comoving wave number. The transfer function, $T(\eta)$, and the damping factor, $D_W(\eta)$, describing the free streaming of DM particles were given in Bardeen et al. (1986).

The correlation function of the initial velocity field is expressed through the power spectrum:

$$\xi_v(l_v q) = \frac{3}{m_{-2}}\int_0^\infty d\eta\,\eta^2\cos x\int_\eta^\infty \frac{dy}{y^2}T^2(y)D_W(y)\,, \tag{5}$$

$$x = kl_v q, \quad \eta = k/k_0, \quad \xi_v(0) = 1, \quad \int_0^\infty dq\ \xi(l_v q) = 0\,.$$

where $l_v q$ is the Lagrangian distance between two DM particles at $z = 0$. For the spectrum (4) the coherent length of velocity field, l_v, is:

$$l_v = \frac{6.6}{\Omega_m h^2}\text{Mpc} \approx 31.4h^{-1}\frac{0.21}{\Omega_m h}\text{Mpc}\,.$$

For the CDM – like spectrum (4) and for the most interesting range $0.5 \geq q$ the velocity correlation function can be fitted by:

$$\xi_v(q) = \xi_{CDM} \approx 1 - \frac{1.5q^2}{\sqrt{2.25q^4 + q^2 + p_0^{1.4}q^{0.6} + q_0^2}}\,, \tag{6}$$

where $p_0 \approx 1.1 \cdot 10^{-2}$, and $q_0 < 10^{-5}$ is expressed through moments of the power spectrum.

3.1.1 Correlation functions derived from absorbers separations

Comparing the theoretical and measured PDFs of absorber separations we can estimate the correlation function of the initial velocity field, $\xi_v(q_{rd})$, where $q_{rd} = d_{sep}/l_v$. This approach uses only the measured redshifts and, so, the derived function does not depend upon the measured $b\,\&\,N_{HI}$ and the model of absorbers.

The reconstructed correlation function $1-\xi_v(q_{rd})$ is plotted in Fig. 3 for the samples of 19 QSOs (6 251 and 7 411 separations) and 14 QSOs (3 660 separations). For these samples we have, respectively,

$$\frac{1-\xi_v(q_{rd})}{1-\xi_{fit}(q_{rd})} \approx 0.95 \pm 0.25, \quad 1 \pm 0.2\,,$$

$$1-\xi_{fit}(q_{rd}) = \frac{1.5q_{rd}^2}{\sqrt{2.25q_{rd}^4 + q_{rd}^2 + p_s^{1.4}q_{rd}^{0.6}}}, \quad p_s = 2.1 \cdot 10^{-3}, \tag{7}$$

$$0.5 \geq q \geq 1.4 \cdot 10^{-3}, \quad 17h^{-1}\text{Mpc} \geq l_v q_{rd} \geq 0.03h^{-1}\text{Mpc}\,.$$

As is seen from Fig. 3, at $q_{rd} \geq 10^{-2}$, $l_v q_{rd} \geq 0.33h^{-1}$Mpc the derived correlation function coincides with the standard CDM – like one (6) for heavy DM particles, with $q_0 \leq 10^{-3}$, $M_{DM} \geq 1$MeV. At small scales, $10^{-3} \leq q_{rd} \leq 10^{-2}$, we see an excess of power with respect to the reference function ξ_v (6). This excess is caused by the deficit of observed absorbers with small separation what increases the derived function.

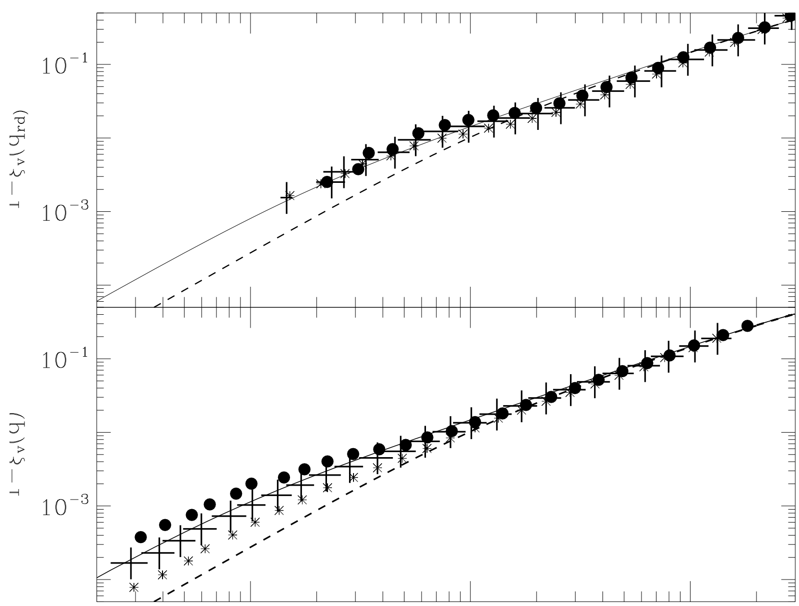

Figure 3: Top panel: the correlation function of initial velocity field, $1 - \xi_v(q_{rd})$, together with the theoretical fits (6) (dashed line) and the fit (7) (solid line). Points and stars show the same functions found for the sample of 14 QSOs and for the sample of 7 411 separations in 19 spectra, respectively. Bottom panel: the correlation function of initial velocity field, $1 - \xi_v(q)$, together with the theoretical fit (6) (dashed line) and the fit (8) (solid line). Points and stars show the same functions found for the sample of 14 QSOs and for the sample of 7 430 separations.

3.1.2 Correlation functions derived from DM column density of absorbers

The correlation function of the initial velocity field, $\xi_v(q)$, can be also found from estimates of the DM column density of absorbers, q. Here we use a more complex procedure of determination of q from the observed $z, b, \& N_{HI}$ and poorly known rate of photoionization, what decreases its reliability. On the other hand, comparison of the functions ξ_v found with two different approaches allows us to test the model of absorbers.

The reconstructed correlation function $1-\xi_v(q)$ is plotted in Fig. 3 for the samples of 19 QSOs with 6 270 and 7 430 absorbers and 14 QSOs (3 674 absorbers). For these samples we have, respectively,

$$\frac{1-\xi_v(q)}{1-\xi_{fit}(q)} \approx 0.95 \pm 0.15, \quad 1.1 \pm 0.2\,,$$

$$1-\xi_{fit}(q) \approx \frac{1.5q^2}{\sqrt{2.25q^4+q^2+p_q^{1.4}q^{0.6}}}, \quad p_q = 0.8\cdot 10^{-3}\,, \tag{8}$$

$$10^{-4} \leq q \leq 0.3, \quad 3h^{-1}\text{kpc} \leq l_v q \leq 9.4h^{-1}\text{Mpc}\,.$$

As is seen from Fig. 3, at $q \leq 5\cdot 10^{-3}$ the derived correlation function (8) differs from the standard CDM – like one (4). For these q both samples of absorbers are quite representative with $N_{abs} \approx 1\,590$ and $N_{abs} \approx 850$ for samples of 19 and 14 QSOs, respectively. However a more complex procedure of determination of ξ_v used now decreases its reliability.

It is important, that similar results are found for both samples of 19 QSOs with 6 270 absorbers and of 14 QSOs with 3 674 absorbers. The samples used are compiled from spectra observed with different instruments and resolutions and the parameters of absorbers were found with different codes what increases their possible non homogeneity. Under these conditions, the stability of our results demonstrates their objectivity.

More detailed discussion of properties of the forest can be found in Demiański & Doroshkevich (2005).

Acknowledgments

This work would not have been possible without the important contribution of M. Rauch and W.L.W. Sargent who provided us with unpublished spectra of five quasars. We are deeply grateful for their permission to use these data. This paper was supported in part by the Polish State Committee for Scientific Research grant Nr. 1-P03D-014-26 and Russian Found of Fundamental Investigations grant Nr. 05-02-16302

References

[1] Bardeen J.M., Bond J.R., Kaiser N., Szalay A., 1986, ApJ., 304, 15

[2] Demiański M. & Doroshkevich A., 2005, astro-ph/0506058

[3] McDonald P. et al., 2004, astro-ph/0405013, astro-ph/0407377

[4] Meiksin A., Bryan G., Machacek M., 2001, MNRAS, 327, 296